

Takuro Hayashi,^a Tetsuya Abe,^b
Kazuki Takeda,^a Nobuhiko
Akiyama,^a Masafumi Yohda^b and
Kunio Miki^{a,c,*}

^aDepartment of Chemistry, Graduate School of Science, Kyoto University, Sakyo-ku, Kyoto 606-8502, Japan, ^bDepartment of Biotechnology and Life Science, Tokyo University of Agriculture and Technology, Koganei, Tokyo 184-8588, Japan, and ^cRIKEN SPring-8 Center at Harima Institute, Koto 1-1-1, Sayo-cho, Sayo-gun, Hyogo 679-5148, Japan

Correspondence e-mail:
miki@kuchem.kyoto-u.ac.jp

Received 30 April 2009
Accepted 17 August 2009

Crystallization and heavy-atom derivatization of StHsp14.0, a small heat-shock protein from *Sulfolobus tokodaii*

Small heat-shock proteins (sHsps) bind and stabilize proteins denatured by heat or other stresses in order to prevent unfavourable protein aggregation. StHsp14.0 is an sHsp found in the acidothermophilic archaeon *Sulfolobus tokodaii*. A variant of StHsp14.0 was crystallized by the sitting-drop vapour-diffusion method. The crystals diffracted X-rays to 1.85 Å resolution and belonged to space group $P2_12_12$, with unit-cell parameters $a = 40.4$, $b = 61.1$, $c = 96.1$ Å. The V_M value was estimated to be $2.1 \text{ \AA}^3 \text{ Da}^{-1}$, assuming the presence of two molecules in the asymmetric unit. Heavy-atom derivative crystals were prepared successfully by the cocrystallization method and are isomorphic to native crystals.

1. Introduction

Small heat-shock proteins (sHsps) are a class of molecular chaperones that are widely found in all domains of life. They are characterized by a relatively small molecular mass in the range 12–43 kDa and by the inclusion of a consensus α -crystallin domain (Haslbeck *et al.*, 2005; Sun & MacRae, 2005). sHsps bind and stabilize proteins denatured by heat or other stresses in order to prevent lethal aggregation. Under nonstress conditions, the hydrophobic sites of sHsps are protected from exposure to the solvent by the formation of oligomers with 12–40 subunits. The oligomer exchanges subunits and dissociates into smaller oligomers under stress conditions (Yang *et al.*, 1999; Shashidharamurthy *et al.*, 2005). The smaller oligomer is presumed to be a dimer based on size-exclusion chromatograms, native PAGE analyses and the large-oligomer structures (Haslbeck *et al.*, 2005). However, the relationship between the oligomer–dimer transition and chaperone activity is not clear.

The structures of two sHsps, MjHsp16.5 from *Methanocaldococcus jannaschii* (Kim *et al.*, 1998) and wHsp16.9 from wheat (van Montfort *et al.*, 2001), have been determined by X-ray crystallography. These sHsps have three common structural regions: the N-terminal region, the α -crystallin domain and the C-terminal region. The α -crystallin domain folds into a compact β -sandwich fold. However, the two sHsps have distinctive oligomeric structures: a 24-mer for MjHsp16.5 and a 12-mer for wHsp16.9 (Kim *et al.*, 1998; van Montfort *et al.*, 2001).

StHsp14.0 was found in the acidothermophilic archaeon *Sulfolobus tokodaii* (Usui, Ishii *et al.*, 2004). Denatured proteins are protected from aggregation by StHsp14.0 at high temperatures of around 360 K (Usui, Ishii *et al.*, 2004; Usui, Hatipoglu *et al.*, 2004). Electron microscopy indicated that StHsp14.0 exists as a 24-meric spherical oligomer like MjHsp16.5 under nonstress conditions, while it forms non-uniformly sized particles in the presence of denatured proteins (Usui, Ishii *et al.*, 2004). A variant of StHsp14.0 termed the FKF variant possesses mutations in the short IXI/V motif at the C-terminus. The FKF variant is primarily a dimer even under nonstress conditions (Saji *et al.*, 2008).

Here, we report the crystallization conditions for the FKF variant of StHsp14.0 from *S. tokodaii*. A successful heavy-atom search using the cocrystallization method is also described.



© 2009 International Union of Crystallography
All rights reserved

2. Materials and methods

2.1. Overexpression and purification

The FKF variant of StHsp14.0 from *S. tokodaii* strain 7 was overexpressed and purified as described previously (Saji *et al.*, 2008). Briefly, transformed *Escherichia coli* strain BL21 (DE3) cells were grown at 310 K in LB medium containing 100 $\mu\text{g ml}^{-1}$ ampicillin. The soluble fractions of disrupted cells were collected and heated at 348 K for 30 min. The supernatant was successively applied onto a DEAE-Toyopearl anion-exchange column (Tosoh, Stuttgart, Germany) and a HiLoad 26/60 Superdex-200 size-exclusion column (GE Healthcare, Uppsala, Sweden). The purified protein was desalted and concentrated with Centriprep YM-10 (Millipore, Bedford, Massachusetts, USA) to approximately 20 mg ml^{-1} in 10 mM Tris-HCl pH 8.0 buffer.

2.2. Crystallization

All crystallization experiments were carried out by the sitting-drop vapour-diffusion method. The initial crystallization trials were performed using several commercial sparse-matrix kits. 0.5 μl protein

solution was mixed with 0.5 μl reservoir solution using a Hydra II crystallization robot (Matrix Technology, Walnut Creek, California, USA) and the resultant drop was equilibrated against 100 μl reservoir solution in a 96-well crystallization plate.

2.3. Heavy-atom derivatization

Heavy-atom derivative crystals were prepared by the cocrystallization method. The compounds examined were manganese chloride, cobalt chloride, sodium bromide, rubidium chloride, strontium chloride, sodium molybdate, sodium iodide, caesium chloride and caesium acetate. Each compound was added to solutions under the above-mentioned crystallization conditions to a final concentration of 10–100 mM. No precipitation was observed in the mixed solutions. For each compound, crystals larger than 0.2 \times 0.2 \times 0.2 mm were used in subsequent data collections.

2.4. X-ray data collection and analysis

Diffraction data for the native crystal were collected on BL38B1 of SPring-8, a third-generation synchrotron-radiation facility (Harima, Japan). The wavelength of the incident X-rays was set to 1.0000 Å. Diffraction data for the heavy-atom derivatives were collected using Cu $K\alpha$ radiation from an in-house MicroMax-007 rotating-anode X-ray generator (Rigaku Co., Tokyo, Japan). A Jupiter-210 CCD detector (Rigaku Co.) was used at the beamline and an R-Axis VII image-plate detector (Rigaku Co.) was used for the in-house experiments. Crystals were picked up with nylon loops (Hampton Research, Laguna Niguel, California, USA) and were transferred into solutions containing an additional 20% (v/v) glycerol as a cryoprotectant. Subsequently, the crystals were frozen in a nitrogen-gas flow generated by a cryocooler (Rigaku Co.). The crystals were maintained at 95–100 K with the cooler during data collection. All diffraction data were processed and scaled using the *HKL-2000* package (Otwinowski & Minor, 1997). Patterson maps were calculated and visualized with the program *XtalView* (McRee, 1999a).

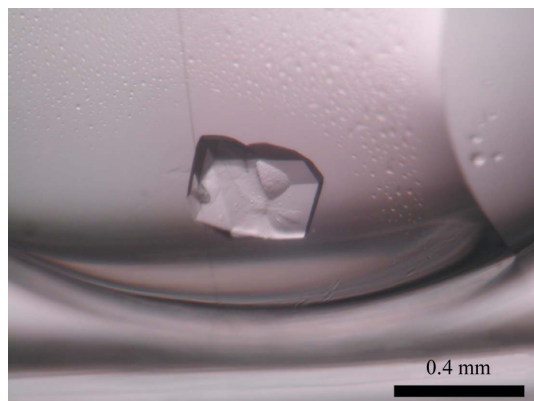


Figure 1
Crystal of the FKF variant of StHsp14.0.

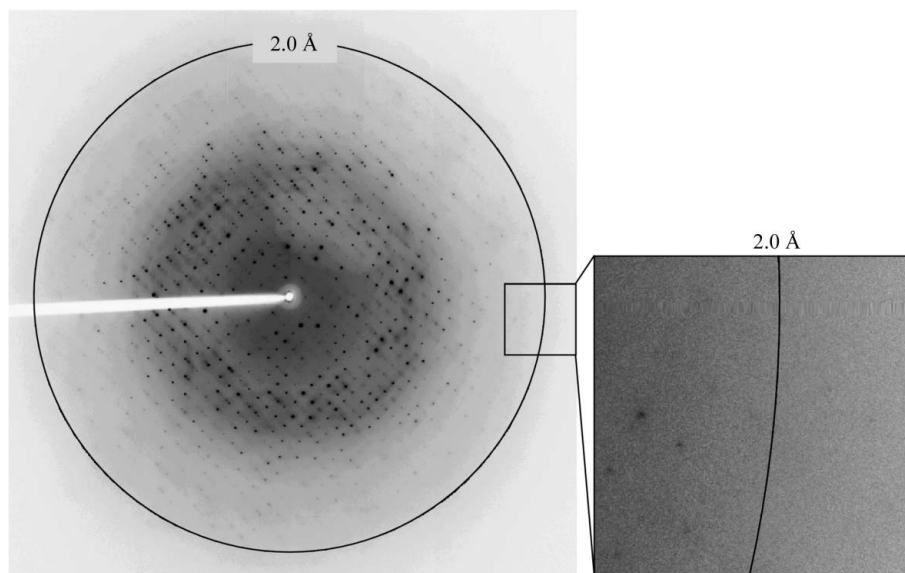


Figure 2
X-ray diffraction image of the native crystal. The close-up view corresponds to the boxed region. The image was recorded using a Jupiter-210 CCD detector (Rigaku Co.) on BL38B1 of SPring-8.

3. Results and discussion

Crystals with dimensions of $0.4 \times 0.2 \times 0.2$ mm (Fig. 1) were obtained in one week using a reservoir solution consisting of 10 mM magnesium chloride, 5.0% (v/v) 2-propanol, 50 mM Tris-HCl pH 7.5 at 290 K. The native crystal diffracted X-rays to 1.85 \AA resolution (Fig. 2) and belonged to space group $P2_12_12$, with unit-cell parameters $a = 40.4$, $b = 61.1$, $c = 96.1 \text{ \AA}$. The crystallographic data and statistics are listed in Table 1. The V_M value is estimated to be $2.1 \text{ \AA}^3 \text{ Da}^{-1}$, assuming the presence of two molecules in the asymmetric unit. This value is consistent with those for protein crystals (Matthews, 1968). The molecular-replacement method with previously reported homologous structures gave no reasonable solutions.

Although all examined heavy-atom compounds gave crystals in our cocrystallization experiments, the crystals obtained using cobalt chloride, rubidium chloride, sodium molybdate, sodium iodide and caesium chloride had sufficient sizes (≥ 0.2 mm in all dimensions) and were suitable for X-ray diffraction analysis. The other compounds provided small and/or clustered crystals. Diffraction data sets were collected from the above five derivatives at resolutions of 2.0–2.5 \AA . All derivative crystals belonged to space group $P2_12_12$. There were only small (0.4–0.7%) differences in the unit-cell parameters between the derivative and native crystals. Strong peaks were found in the Harker sections of the Patterson maps of the rubidium chloride and sodium iodide derivatives (Fig. 3). High isomorphism to the native

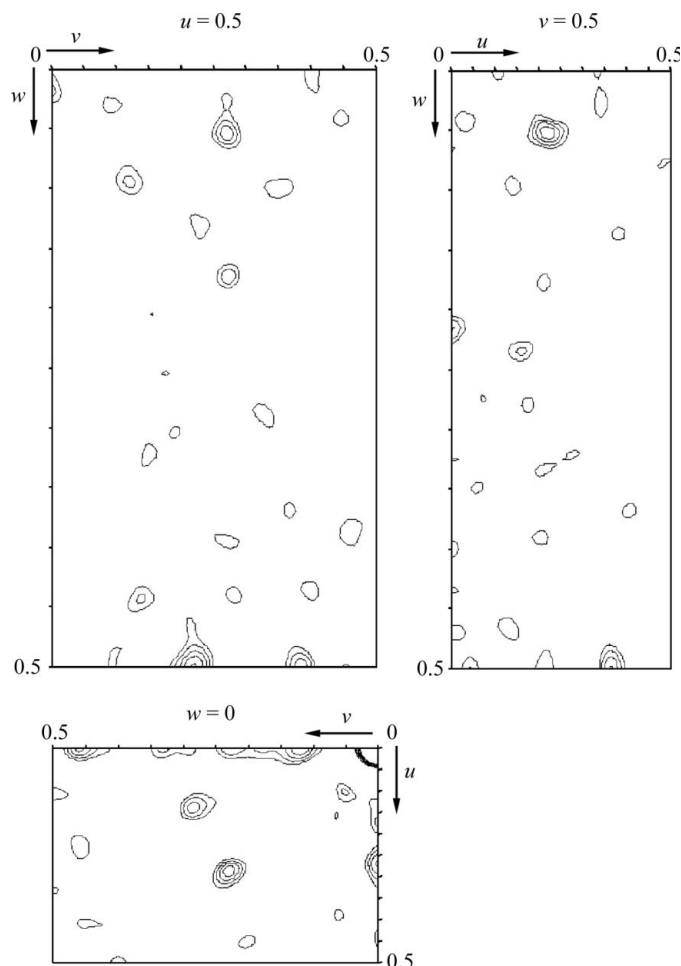


Figure 3 Three Harker sections ($u = 0.5$, $v = 0.5$ and $w = 0$) of the isomorphous difference Patterson map of the rubidium derivative. The contour level is 2σ , with 1 σ increments.

Table 1

Data-collection and crystallographic statistics.

Values in parentheses are for the highest resolution shell.

Data set	Native	Rb	I
Compound	—	Rubidium chloride	Sodium iodide
Concentration (mM)	—	50	100
X-ray source	BL38B1	MicroMax-007	MicroMax-007
Wavelength (\AA)	1.0000	1.5418	1.5418
Detector	Jupiter-210	R-Axis VII	R-Axis VII
Temperature (K)	100	95	95
Space group	$P2_12_12$	$P2_12_12$	$P2_12_12$
Unit-cell parameters (\AA)			
a	40.4	40.3	40.1
b	61.1	60.9	60.8
c	96.1	95.9	95.7
Resolution range (\AA)	40.0–1.85 (1.97–1.85)	40.0–2.00 (2.07–2.00)	40.0–2.10 (2.18–2.10)
Observed reflections	116627	128740	113066
Unique reflections	20341	15194	13347
Redundancy	5.7 (3.3)	8.5 (2.6)	8.5 (3.2)
$I/\sigma(I)$	37.1 (3.0)	54.9 (4.9)	61.8 (7.2)
Completeness (%)	96.8 (92.3)	91.5 (60.6)	93.6 (69.0)
R_{merge} (%) [†]	3.9 (28.5)	5.4 (22.9)	4.8 (19.4)
R_{iso} (%) [‡]	—	19.6	19.3

$$\dagger R_{\text{merge}} = \frac{\sum_{hkl} \sum_i |I_i(hkl) - \langle I(hkl) \rangle|}{\sum_{hkl} \sum_i I_i(hkl)} \quad \ddagger R_{\text{iso}} = \frac{\sum_{hkl} |F_{\text{deriv}}(hkl)| - |F_{\text{native}}(hkl)|}{\sum |F_{\text{native}}(hkl)|}$$

crystal was observed even in these derivatives (Table 1). On the other hand, no clear peaks were observed in the Patterson maps of the other derivatives (data not shown). Interestingly, the Patterson maps for the rubidium chloride and sodium iodide derivatives indicate that the rubidium and iodide ions are located in the same positions in the unit cell despite their difference in charge.

Preparation of heavy-atom derivatives is one of the most laborious steps in protein X-ray crystallography. Therefore, many sets of heavy-atom compounds have been proposed and recommended in order to perform efficient surveys (McPherson, 1982; McRee, 1999b; Boggon & Shapiro, 2000; Morth *et al.*, 2006). Toxic compounds of platinum and mercury and radioactive compounds of uranium are frequently included in the lists. These are usually introduced into protein crystals by soaking or dialysis methods. It is commonly believed that cocrystallization often results in non-isomorphism and it therefore remains unutilized. However, our experience would suggest otherwise. Moreover, the single-wavelength or multi-wavelength anomalous dispersion (SAD or MAD) methods with tunable synchrotron X-rays can solve the phase problem even in the cases of non-isomorphism. Therefore, the cocrystallization method should be further utilized in the preparation of heavy-atom derivatives of protein crystals.

We would like to express our gratitude to the beamline staff at SPring-8. This work was supported in part by the National Project on Protein Structural and Functional Analysis (KM and MY) and the Target Protein Research Program (KM) from the Ministry of Education, Culture, Sports, Science and Technology (MEXT), Japan.

References

- Boggon, T. J. & Shapiro, L. (2000). *Structure*, **8**, R143–R149.
 Haslbeck, M., Franzmann, T., Weinfurter, D. & Buchner, J. (2005). *Nature Struct. Mol. Biol.* **12**, 842–846.
 Kim, K. K., Kim, R. & Kim, S.-H. (1998). *Nature (London)*, **394**, 595–599.
 Matthews, B. W. (1968). *J. Mol. Biol.* **33**, 491–497.
 McPherson, A. (1982). *Preparation and Analysis of Protein Crystals*. New York: John Wiley & Sons.
 McRee, D. E. (1999a). *J. Struct. Biol.* **125**, 156–165.

- McRee, D. E. (1999b). *Practical Protein Crystallography*, 2nd ed. San Diego: Academic Press.
- Montfort, R. L. van, Basha, E., Friedrich, K. L., Slingsby, C. & Vierling, E. (2001). *Nature Struct. Biol.* **8**, 1025–1030.
- Morth, J. P., Sørensen, T. L. & Nissen, P. (2006). *Acta Cryst.* **D62**, 877–882.
- Otwinowski, Z. & Minor, W. (1997). *Methods Enzymol.* **276**, 307–326.
- Saji, H., Iizuka, R., Yoshida, T., Abe, T., Kidokoro, S., Ishii, N. & Yohda, M. (2008). *Proteins*, **71**, 771–782.
- Shashidharamurthy, R., Koteiche, H. A., Dong, J. & McHaourab, H. S. (2005). *J. Biol. Chem.* **280**, 5281–5289.
- Sun, Y. & MacRae, T. H. (2005). *Cell. Mol. Life Sci.* **62**, 2460–2476.
- Usui, K., Hatipoglu, O. F., Ishii, N. & Yohda, M. (2004). *Biochem. Biophys. Res. Commun.* **315**, 113–118.
- Usui, K., Ishii, N., Kawarabayashi, Y. & Yohda, M. (2004). *Protein Sci.* **13**, 134–144.
- Yang, H., Huang, S., Dai, H., Gong, Y., Zheng, C. & Chang, Z. (1999). *Protein Sci.* **8**, 174–179.